Open Access **Baghdad Science Journal** **P-ISSN: 2078-8665**
Published Online First: January, 2023 **2023, 20(4): 1283-1296** **E-ISSN: 2411-7986**

DOI: https://dx.doi.org/10.21123/bsj.2023.7066

Kinetic and Theoretical Study of Removal Gentian Violet from Aqueous Solution Using Stachy Plant

Zhahraa A. Mahmood* ***Ahlam M Farhan*** ***Nafeesa J Kadhim*** ***Muna S Hade***

Department of Chemistry, College of Science for Woman, University of Baghdad, Baghdad, Iraq.
*Corresponding author: zahraaam_chem@csw.uobaghdad.edu.iq
E-mail addresses: ahlammfchem@csw.uobaghdad.edu.iq , nafeesa.j1975@gmail.com , 38sameer@gmail.com

Received 17/2/2022, Revised 24/6/2022, Accepted 26/6/2022, Published Online First 20/1/2023, Published 1/8/2023

Abstract:

The main parameters and methods influencing the removal of Gentian Violet (GV) dye from aqueous media were investigated using a stachy plant in this study. The surface of the stachy plant was determined using FTIR spectra. Adsorption is influenced by the adsorbent's characteristic groups. The research took into account the usual conditions for GV dye adsorption by the stachy plant, such as the impact of contact time. Mass dosage , after 0.3 g the amount of adsorbed dye declines. Study pH and ionic strength, the results obtained showed that at pH 3 the largest adsorption of (GV) was seen, while at pH 9, the lowest adsorption was observed at 298 K, the adsorption kinetics and equilibrium constants were achieved, and the equilibrium data was fitted using the Langmuir, Freundlich, and Temkin models. The pseudo-first-order and pseudo-second-order kinetic models were used to investigate the adsorption process of gentian violet. The adsorption kinetics was discovered to be governed by a pseudo-second-order kinetic model with a determination coefficient (R^2) of 0. 0.9943. Study the theoretical electrostatics of Gentian Violet dye was measured and plotted as a 2D and 3D contour and the program hyperchem-8.07 was used for semi-empirical and molecular mechanic calculations in the gas phase to estimate the total energy.

Keywords: Adsorption, Gentian Violet, kinetic, Stachy plant, Temkin models.

Introduction:

Textiles, paper, printing, leather, food, cosmetics, and other sectors that utilize dyes to color their end product consume a lot of water. Dye-containing wastewater is very difficult to handle since the dyes are recalcitrant organic molecules that are resistant to aerobic digestion and light stability. Dyes, even at very low concentrations, are highly visible and cause environmental harm because they are harmful to marine life [1]. Suspended elements, mineral solutes, organic solutes, dissolved gases, and microbes are only a few of the most prevalent types of water pollutants. Because of their commercial and societal importance, the effects and toxicity of important dyes discharged into the atmosphere have been intensively investigated [2]. Synthetic dyes are particularly harmful to all forms of life since they contain sulfur, colors, nitrates, acetic acid, surfactants, enzymes, chromium compounds, and heavy metals like copper, arsenic, silver, cadmium, mercury, nickel, cobalt, and a few more substances. Violet 3 (Basic) the synthetic cationic dyes, gentian violet, and methyl violet 10B all belong to the triarylmethane group. This dye is commonly used to dye cotton, wool, silk, and nylon in the textile industry, as well as in the creation of printing inks and as a dermatological agent in biological stains and veterinary medicine [3]. Gentian violet (GV) is toxic and it can cause discomfort when absorbed through the skin, as well as inhalation and ingestion. It can cause kidney failure and eye inflammation, which can lead to permanent blindness and cancer in serious cases [4]. As a result, removing GV from wastewater is extremely important. Inhalation, ingestion, and direct contact with the skin are all ways that gentian violet dye (GV) can affect humans, causing cancer and extreme eye irritation [5].

Adsorption is one of the most efficient dye removal methods, less expensive and harmless absorbent materials should be used in the adsorption process. Many low-cost adsorbents derived from agricultural wastes and natural materials have recently been investigated for dye removal from aqueous solutions [6] . Researchers have published a study that focuses on low-cost adsorbents that are mostly obtained from agricultural waste and industrial leftovers since they are abundant in nature and require minimal processing. Plant waste is cheap because it has no or very little economic value. This has led many workers to search for the use of cheap and efficient alternative materials. As a result, many employees are looking for low-cost, high-efficiency alternatives [7]. Spent corncob substrate [8], sunflower seed shells [9], palm kernel fiber [10], Luffa cylindrical fibers [8], olive pomace [11], Biologically Active Plants[12], wheat shells [13] and pomelo (Citrus grandis) peel. The aim of this research is to determine the stachys plant's static adsorption ability of Gentian Violet (G).

Materials and Methods:

Adsorbent

The plant Stachys was used in this analysis, distilled water was used to clean the plant leaves. The plant leaves were then filtered before being dried in a 60°C oven for 4 hours to remove any remaining moisture and leave it for a week at room temperature. The dried materials were ground and sieved to a size of 150 microns to make powder. The stachys plant sample that has been prepared.

Adsorbate

To make the stock solution, 0.1 g of (GV) was dissolved in 1 L distilled water. It was slowly soaked to ensure that all of the (GV) powder was dissolved in distilled water. The experimental solutions were made by accurately diluting the dye stock solution to various initial concentrations ranging from (1- 5) ppm, with a maximum wavelength of 590 nm for (GV). This dye's structure is listed in Fig. 1.

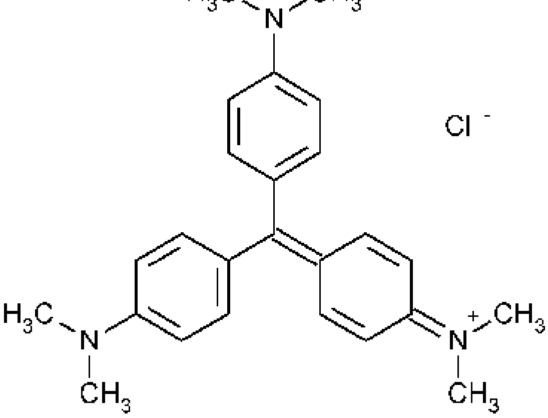

Figure 1. The structure of Gentian Violet

Adsorption in batch mode:

Adsorption tests were carried out in a rotary shaker with dye solutions in round bottom glass flasks. Each flask was filled with a fixed amount of adsorbent and then sealed. At the maximum wavelength (590 nm), the concentrations of dye samples were measured. Using a Shimadzu UV-VIS Spectrophotometer and a normal calibration curve per experiment, all measurements were made in triplicate. The following equations are used to measure the sum of GV adsorbed onto stachys and the removal efficiency R [6]:

$$Q_e = (C_o - C_e)\ V / W \qquad 1$$

C_o and C_e are the initial and equilibrium concentrations (mg/L) of GV in solution. The amount of GV adsorbed on the adsorbent at equilibrium (mg/g), the volume of solution (L), and (W) the mass of adsorbent (g).

The effect of different parameters of adsorption processes of GV:

The influence of contact time

Adsorption equilibrium trials using 0.3 g of adsorbent in 75 mL of dye at a concentration of 5 ppm are carried out at 25°C for 5, 10, 15, 20, and 25 minutes.

The Effect of mass dosage

The effect of mass dose was examined by agitating in different masses (0.1, 0.2, 0.3, 0.4, and 0.5 g) at 25 °C, 100 rpm, and 75 mL of (GV) dye concentration 5 ppm.

The Effect of pH

At 25 °C, 100 rpm, and 75 mL of dye concentration 5 ppm. At various pH levels, the influence of pH on the rate of color loss was examined (3, 5, 7, and 9). 0.1 N NaOH and 0.1 N HCl solutions were used to adjust the pH using a pH meter with a composite pH electrode.

The Effect of ionic strength

Adsorption studies were performed at 25 °C using 75 mL of dye with a 5 ppm concentration and varied KCl concentrations (0.01, 0.001, 0.0001) M.

Results and Discussion:

Surface Characterizations

The adsorbent deposit of Stachys was investigated using Fourier Transform Infrared spectroscopy (FTIR), with spectra taken before and after Gential Violet concentration 5 ppm adsorptions shown in Figs. 2 and 3.

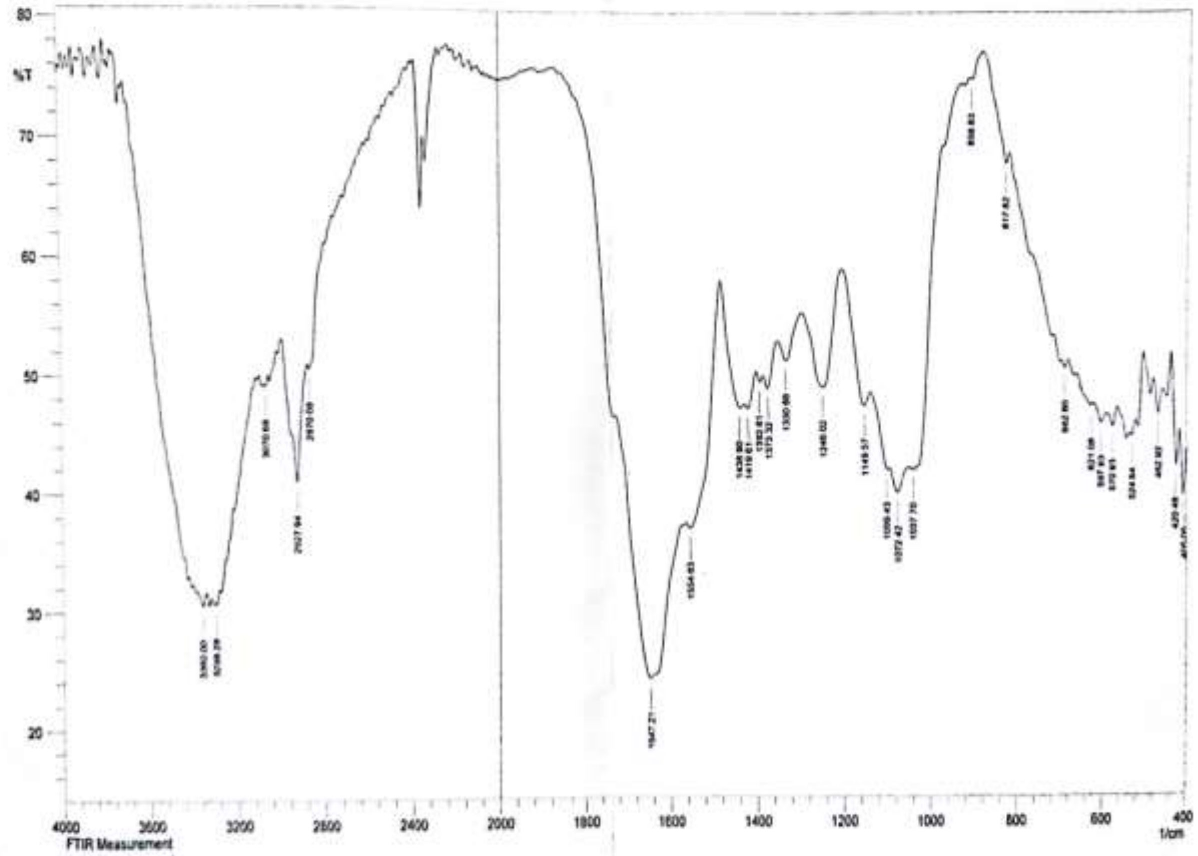

Figure 2. FTIR spectrum of stachys deposit

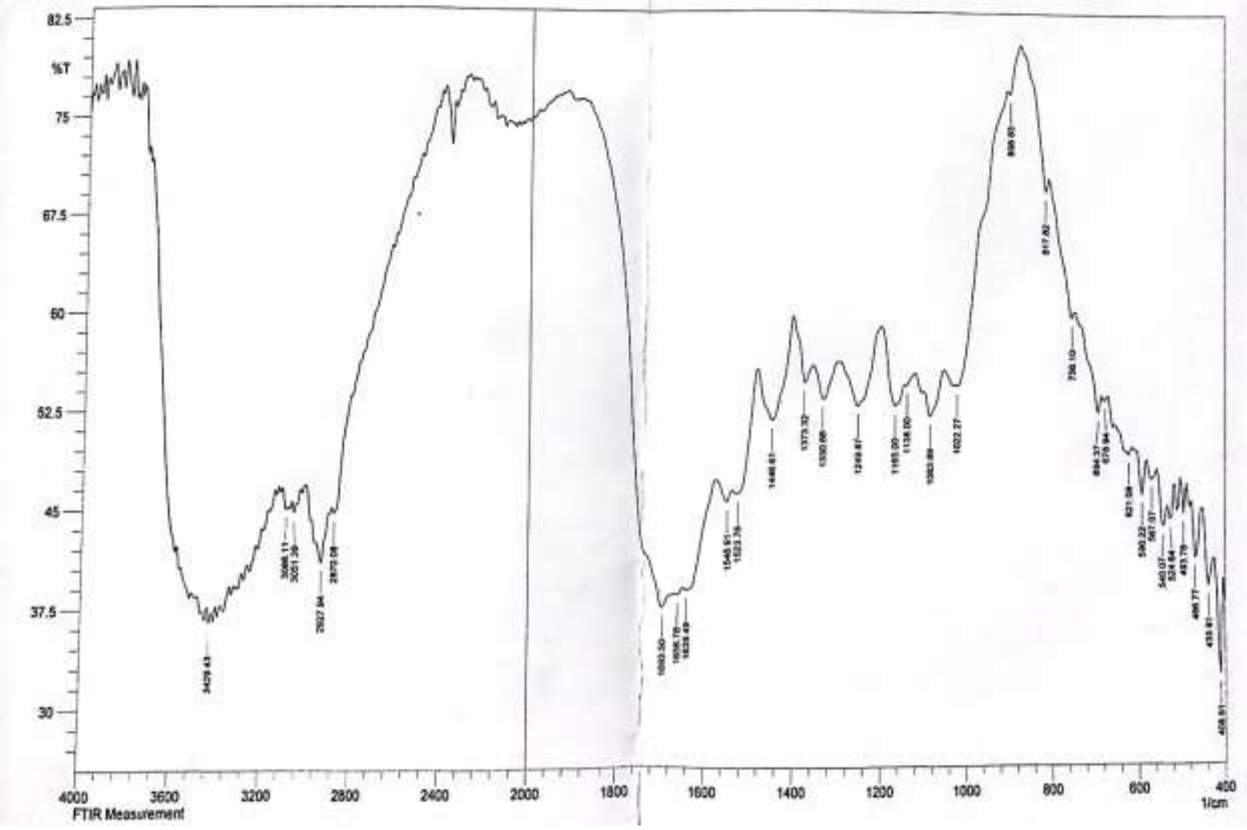

Figure 3. FTIR spectrum of stachy plant deposit with Gential Violet at concentration 5 ppm

We can see absorption bundles from the OH- hydroxyl groups in the range (3429.43- 3417.86 cm^{-1}) and the appearance of absorption bundles at (3082.25- 3074.53 cm^{-1}) after adsorption returns to the aromatic CH groups in the dye and C = C groups at (1647.21 cm^{-1}), C = O groups at (1680–1630 cm^{-1}) in the FTIR spectrum the CH-groups on the surface of the stachys powder, as well as the active N-H group within the range, account for the absorption in this range (2924.04-2920.23 cm^{-1}) (1249.78 cm^{-1}). These groups are important sites for adsorption since they have the ability to shape chemical or physical bonds and can include a pair of electronic or electrostatic changes that can be involved in the formation of physical links or chemical bonds[14].

The Effect of Contact Time

Figure 4 depicts the influence of contact time on the adsorption of (GV) onto stachys. The results show that the adsorption process reached equilibrium in 25 minutes, and that the amount of dye removed at equilibrium increased as contact time increased. After 15 minutes, the changes in equilibrium adsorption became more stable, and equilibrium was reached in 25 minutes. The adsorbent's ability gradually depleted over time as the few remaining vacant surface sites became difficult to occupy due to repulsive forces between the solute molecules on the solid and bulk phases, and the high removal rate at the start of the contact period was due to the large amount of surface area available for dye adsorption during the initial stage.[12]

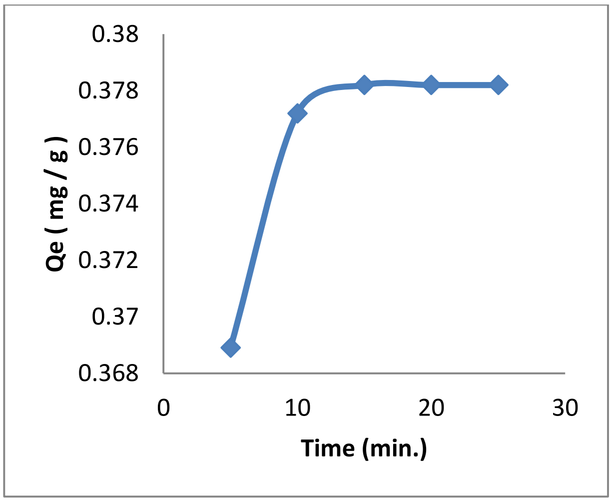

Figure 4. The effect of contact time on the adsorption of Gentian Violet dye.

The Effect of Adsorbent Dosage

Figure 5 shows the adsorption of dye GV as a function of adsorbent dosage. The amount of adsorbed dye increases as the adsorbent dose is increased, but the adsorption quantity decreases after 0.3 g. It is self-evident that raising the adsorbent dose increases the number of usable adsorption sites, resulting in an increase in the amount of adsorbed material dye [15]. The decrease in adsorption density as the adsorbent dose is increased is due to the fact that adsorption sites remain unsaturated during the adsorption reaction, while the number of adsorption sites available increases as the adsorbent dose is increased [16].

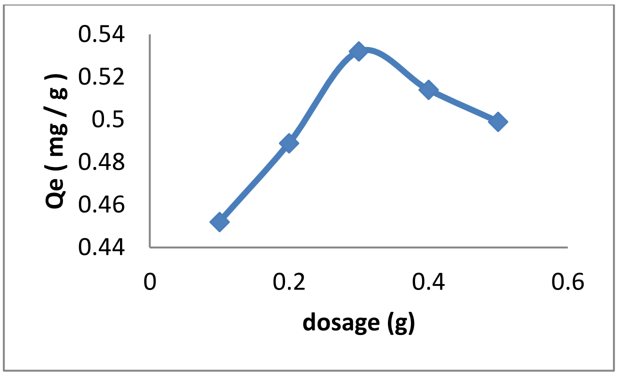

Figure 5. The Effect of adsorbent dosage on the removal of Gentian Violet dye

Determination of Adsorption Isotherm Parameters:

The adsorption isotherm can be used to define the dye distribution between the solid phase and the solution at a specific temperature once equilibrium has been attained. The Langmuir, Freundlich, and Temkin models were employed to fit the equilibrium data. Fig. 6 shows that the adsorption of GV dye on the surface of the stachy follows the pattern (S3), and the orientation of the adsorbed molecules on the adsorbing surface is in an oblique or vertical manner.

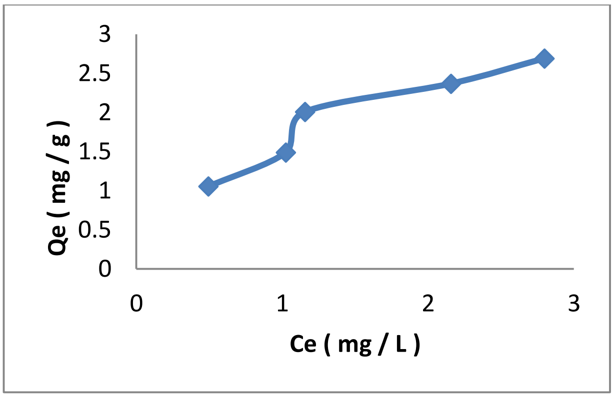

Figure 6. Adsorption isotherms of GV on stachy at (25) °C

Langmuir Isotherm

The Langmuir isotherm theory assumes that the adsorbate is coated in a monolayer on a homogeneous adsorbent surface. A plateau characterizes the Langmuir isotherm graphically. As a result, the saturation point is achieved at equilibrium, at which no additional adsorption may occur. Adsorption occurs at specified spots on the homogenous surface of the adsorbent. There can be no adsorption once a dye molecule has occupied a spot. The Langmuir isotherm has a well-known linear expression, as shown below [17]:

$$C_e / Q_e = 1 / Q_m \; k_L + C_e / Q_m \qquad 2$$

where Ce stands for equilibrium concentration (mg/L), Q_e stands for equilibrium amount adsorbed (mg/g), and Q_m and k_L stand for the Langmuir constants for adsorption efficiency and energy, respectively. The Langmuir isotherms are applicable based on the linear plots of C_e / Q_e vs C_e Fig. 7. Table 1 shows the values of Q_m and k_L calculated from the slope and intercepts (1).

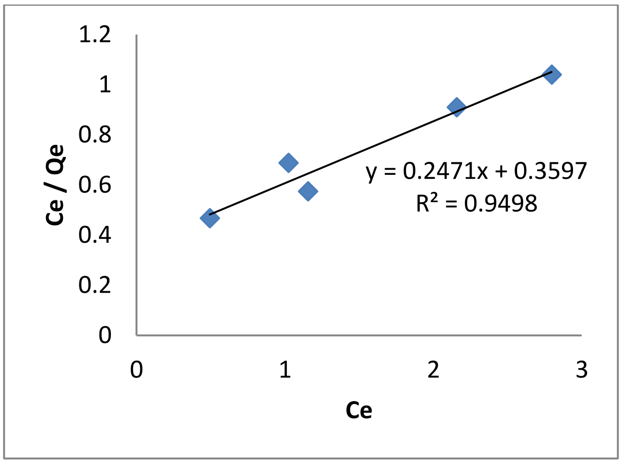

Figure 7. The linear plot of Langmuir isotherms

Freundlich Isotherm

The Freundlich isotherm is an empirical equation that applies to adsorption on heterogeneous surfaces and is not restricted to the generation of monolayers. The amount of adsorbate adsorbed on the adsorbent surface is thought to increase as the adsorbate concentration rises. The Freundlich isotherm can be represented in its linear form as follows[18].:

$$\log Q_e = \log K_f + 1/n \log C_e \qquad 4$$

where Q_e is the total amount of Gentian violet dye adsorbed (mg/g), C_e is the equilibrium dye concentration in solution (mg/L), and K_f and 1/ n are constants that integrate the adsorption ability and strength, respectively. The adsorption of (GV) dye is shown by linear plots of log Q_e versus log C_e. Fig. 8 shows the Freundlich adsorption isotherm. The values of K_f and 1/n given in Table 1.

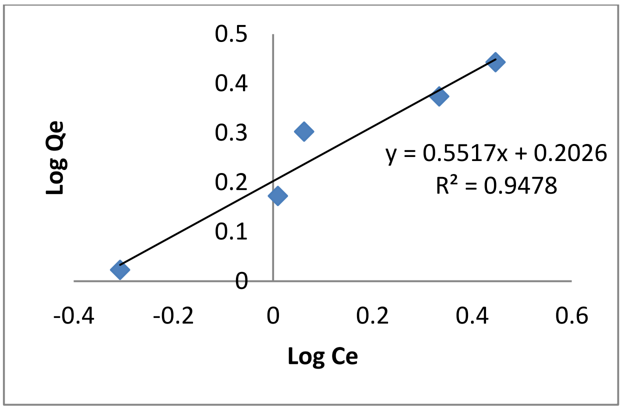

Figure 8. The linear plot of Freundlich isotherms

Temkin Isotherm

Temkin and Pyzhev looked into the impact of specific indirect sorbate/adsorbate interactions on adsorption isotherms, proposing that as a result of these interactions, the heat of adsorption of all molecules in the layer will drop linearly with coverage [19]. The Temkin isotherm was used in the following applications:

$$q_e = RT / \; b \ln (K_T C_e) \qquad 5$$

K_T stands for the equilibrium binding constant (L/g), b for the heat of adsorption (J/mol), R for the universal gas constant (8.314J/mol K), and T for the absolute temperature (K), As shown in table 1 . Fig. 9 shows the Temkin adsorption isotherm. When plotting q_e against ln C_e, the values of the constants b, k_T are obtained from the slope and intercept values.

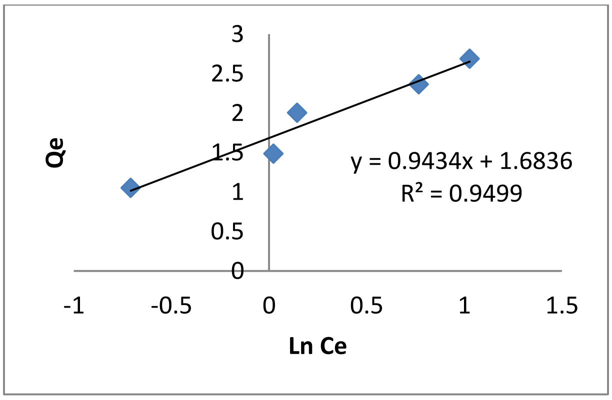

Figure 9. Temkin isotherms plotted in a linear fashion.

Table 1. The parameters of the Freundlich, Langmuir, and Temkin equations for the adsorption of GV on stachy .

	Freundlich parameter		
T (°C)	**n**	**K_F**	**R^2**
25	**1.8125**	**1.2245**	**0.9478**
	Langmuir parameter		
T (°C)	**Q_m**	**K_L**	**R^2**
25	**0.6869**	**2.7800**	**0.9498**
	Temkin parameter		
T (°C)	**b**	**K**	**R^2**
25	**0.943**	**1.6836**	**0.9499**

Through the results of Table 1, it was found that the adsorption of GV dye is in great agreement with an equation Temkin.

The Effect of pH:

The effect of pH on the adsorption of (GV) was examined at pH 3, 5, 7, and 9. At pH 3, the largest adsorption of (GV) was seen, while at pH 9, the lowest adsorption was observed (see Fig. 10). As the pH of the solution increased [20, 21], the adsorption of (GV) decreased. This was due to the extinction of the positive hydrogen ions, which encouraged electrostatic repulsion between the negative charges of the dye surface [22]. The carboxylic groups are the most prevalent at an acidic pH [23]. The surface charge of stachys becomes more positively charged at pH 3, boosting (GV) adsorption via electrostatic attraction. Fig.10 shows the results of the pH effect on Gentian violet elimination.

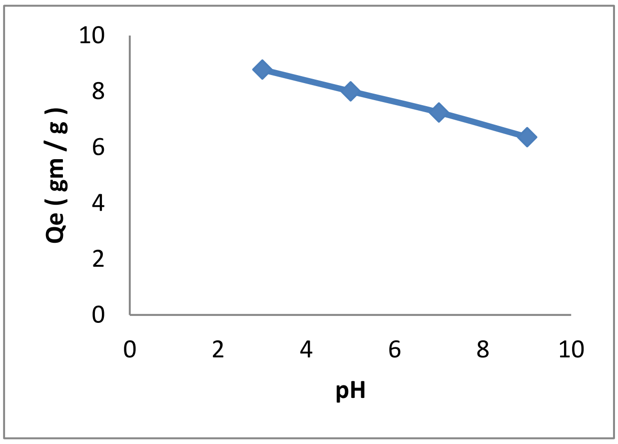

Figure 10. The effect of pH on the elimination of (GV) at a pH of 5. (ppm).

The Effect of Ionic Strength:

Because large amounts of salts are routinely employed in the dyeing process, the influence of ionic strength on adsorption was investigated in this study. The concentrations of KCl in the solution (0.01, 0.001, 0.0001) M and were varied to see what happened. The increase in adsorption with increased ionic strength could be due to compression of the thickness of the diffused double layer. The reason this is due to the fact that the interactions between the solvent molecules and KCl ions are higher than the interactions of the dye which leads to an increase in the solubility of the dye in the aqueous solution, and thus leads to an increase in the solubility of the dye in the aqueous solution in the ability to be adsorbed on the surface. The adsorbent particle and adsorbate species may be aided in approaching each other more closely as a result of the compression, resulting in considerable attractive forces and enhanced adsorption[24]. Fig. 11 shows the Effect of ionic strength on removal of Gentian Violet.

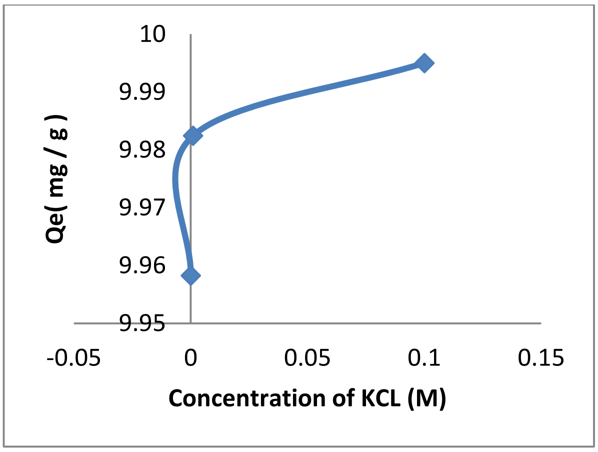

Figure 11. The Effect of ionic strength on removal of Gentian Violet

Adsorption Kinetics Modeling:

The kinetics of adsorption is crucial for controlling the efficiency of a process. Various kinetic models, including pseudo-first-order and pseudo-second-order models, have been studied by various researchers. The kinetics of adsorption is significant because it regulates the efficiency of the process. Lagergren's pseudo-first-order rate equation is roughly defined by the following equation[16]:

$$\log (q_e - q_t) = \log q_e - (k / 2.303\, t) \qquad 6$$

q_e is the total amount of dye adsorbed at equilibrium in mg/g. Plotting log (q_e - q_t) versus t for various dye concentrations yielded the value of k. . Fig. 12 shows the Pseudo - first order plot for (GV) dye adsorption.

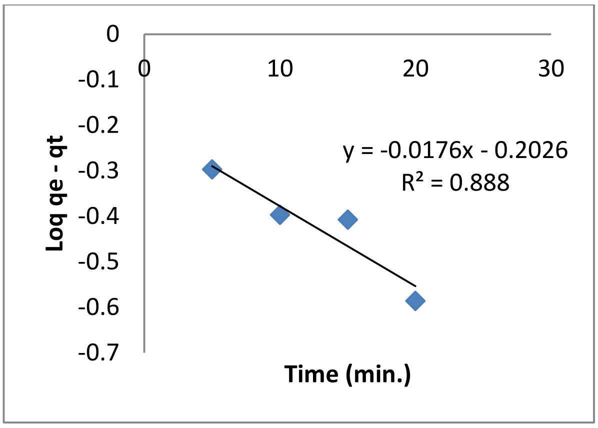

Figure 12. Pseudo - first order plot for (GV) dye adsorption.

The pseudo-second-order kinetic model the following equation [16]:

$$t/ q = 1 / k_2 q_e^{2} + t/ q_e \qquad 7$$

A linear relationship is obtained by plotting t/q vs t, where k_2 is the second-order rate constant (g/mg min). The k_2 and q_e values the intercept and slope of the plots of t/q versus t is determined. Fig. 13 shows the Pseudo-second order plot of (GV) dye adsorption.

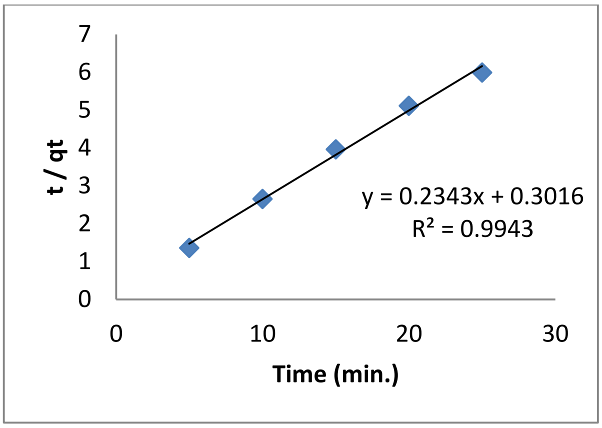

Figure 13. Pseudo-second order plot of (GV) dye adsorption.

In this study, the adsorption of Gentian Violet by stachy plants was explained using the pseudo-second order model. The second-order kinetic model had higher correlation coefficients than the first-order kinetic model[25].

Theoretical Studies:

a) Theoretical electrostatics (potential energy) (E.P) The electron distribution is important for locating reaction sites in a molecule because it determines the electrostatic potential of molecules and specifies the interaction of the molecular system's energy with a positive point charge. A molecule having a substantially negative electrostatic charge is more likely to be attacked by positively charged species [26]. To examine the reactive sites of the molecules, the (E.P) of Gentian Violet dye was measured and plotted as a 2D and 3D contour, fig. 14.

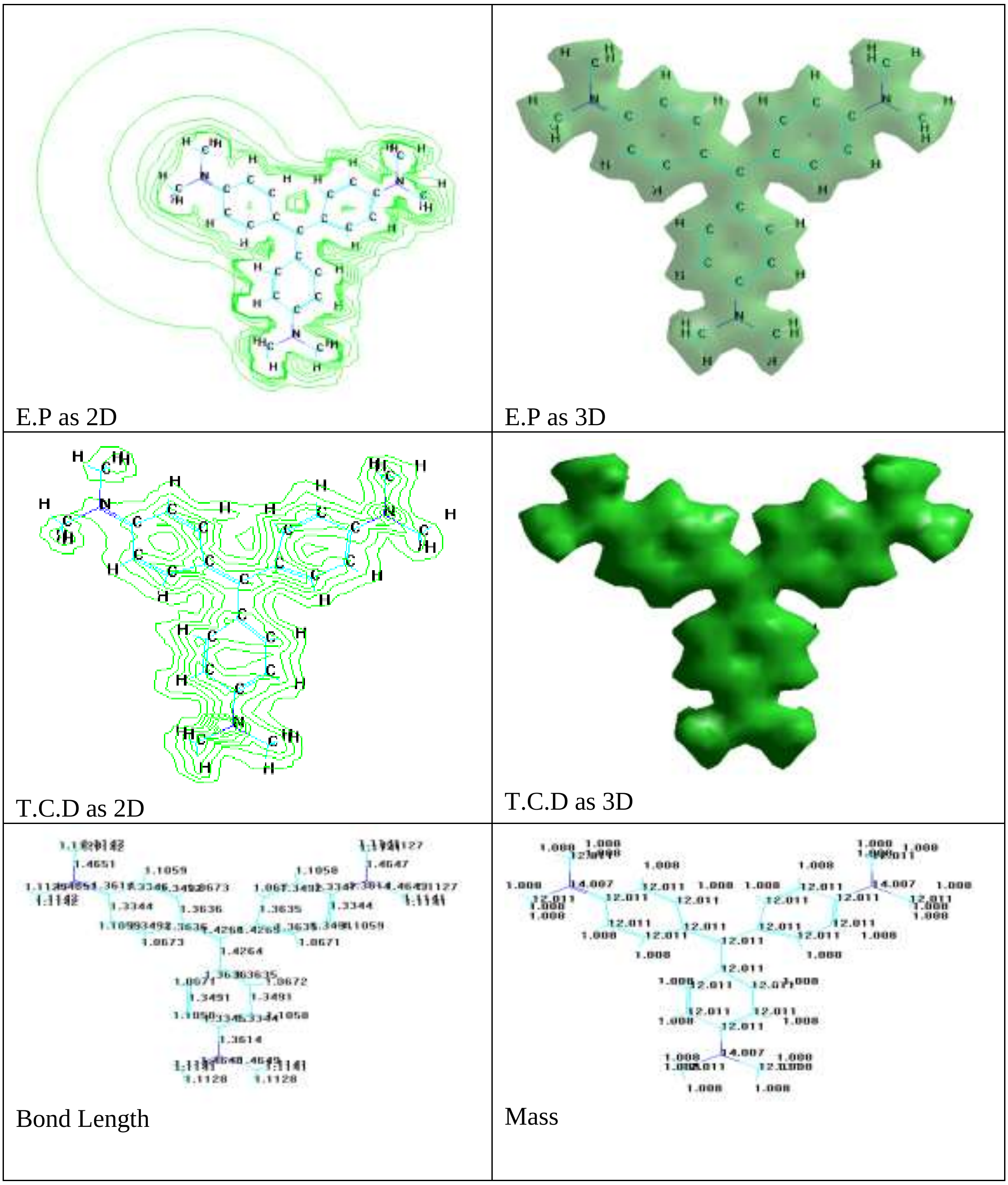

E.P as 2D

E.P as 3D

T.C.D as 2D

T.C.D as 3D

Bond Length

Mass

Figure 14. Electrostatic Potential and Total charge density of Gentian Violet dye

b) The program hyperchem-8.07 was used for semi-empirical and molecular mechanic calculations in the gas phase to estimate the total energy (ET) 30.3449 (Kcal/mol) and dipole moment of 0.0383 Debye's for the Gentian Violet dye, which were calculated using the (PM3) method at 298 K and a value of geometry optimization constant (0.01 Kcal/ mol). Fig.15 shows Conformation Structure of Gentian Violet dye Using Hyperchem. -8.07 Program, and table (2, 3) shows bond length of Gentian Violet dye and dihedral angles of Gentian Violet dye.

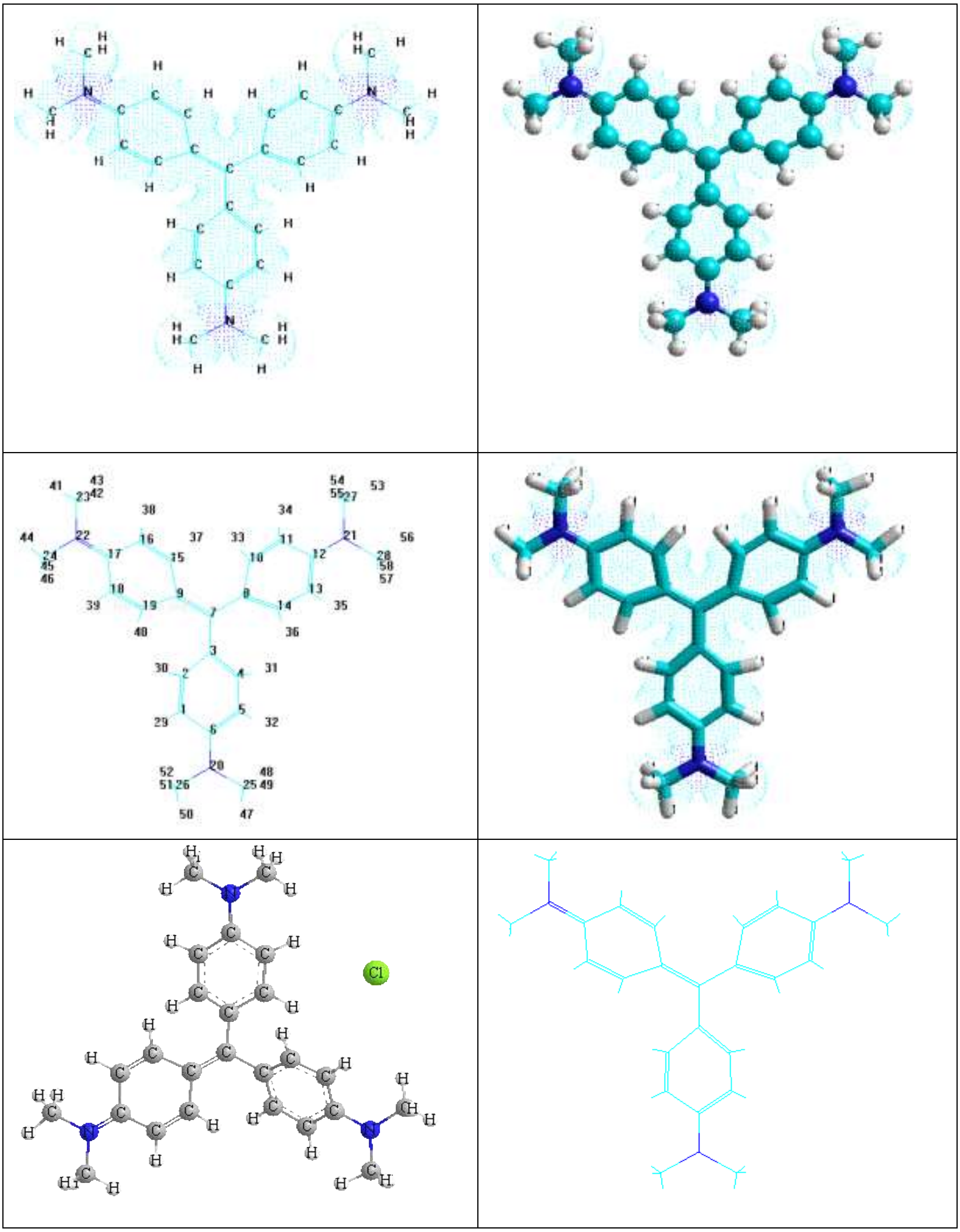

Figure 15. Conformation Structure of Gentian Violet dye Using Hyperchem.-8.07 Program.

Table 2. bond length of Gentian Violet dye.

Bond	Actual (Aº)	Optimal(Aº)	Bond	Actual (Aº)	Optimal(Aº)
C(28)-H(59)	1.113	1.1131	N(21)-C(28)	1.47	**1.4799**
C(28)-H(58)	1.113	1.1153	N(21)-C(27)	1.47	**1.4817**
C(28)-H(57)	1.113	1.1126	N(20)-C(26)	1.47	**1.4835**
C(27)-H(56)	1.113	1.116	N(20)-C(25)	1.47	**1.4831**
C(27)-H(55)	1.113	1.1136	N(22)-C(24)	1.5	**1.5218**
C(27)-H(54)	1.113	1.1117	N(22)-C(23)	1.5	**1.5253**
C(26)-H(53)	1.113	1.114	C(17)-N(22)	1.3	**1.3396**
C(26)-H(52)	1.113	1.1135	C(12)-N(21)	1.462	**1.4396**
C(26)-H(51)	1.113	1.1059	C(6)-N(20)	1.462	**1.4261**
C(25)-H(50)	1.113	1.1135	C(19)-C(9)	1.503	**1.4676**
C(25)-H(49)	1.113	1.1142	C(18)-C(19)	1.337	**1.3534**
C(25)-H(48)	1.113	1.1075	C(17)-C(18)	1.503	**1.4674**
C(24)-H(47)	1.113	1.1137	C(16)-C(17)	1.503	**1.4685**
C(24)-H(46)	1.113	1.1138	C(15)-C(16)	1.337	**1.3562**
C(24)-H(45)	1.113	1.1082	C(9)-C(15)	1.503	**1.4717**
C(23)-H(44)	1.113	1.1134	C(14)-C(8)	1.42	**1.408**
C(23)-H(43)	1.113	1.1123	C(13)-C(14)	1.42	**1.3963**
C(23)-H(42)	1.113	1.1131	C(12)-C(13)	1.42	**1.4088**
C(19)-H(41)	1.1	1.1011	C(11)-C(12)	1.42	**1.4065**
C(18)-H(40)	1.1	1.1016	C(10)-C(11)	1.42	**1.3993**
C(16)-H(39)	1.1	1.1015	C(8)-C(10)	1.42	**1.4044**
C(15)-H(38)	1.1	1.1002	C(7)-C(9)	1.337	**1.3813**
C(14)-H(37)	1.1	1.1071	C(7)-C(8)	1.503	**1.5063**
C(13)-H(36)	1.1	1.103	C(3)-C(7)	1.503	**1.4844**
C(11)-H(35)	1.1	1.1026	C(6)-C(1)	1.42	**1.4104**
C(10)-H(34)	1.1	1.1074	N(21)-C(28)	1.42	**1.4138**
C(5)-H(33)	1.1	1.0999	N(21)-C(27)	1.42	**1.3938**
C(4)-H(32)	1.1	1.0989	C(3)-C(4)	1.42	**1.4104**
C(2)-H(31)	1.1	1.1011	C(2)-C(3)	1.42	**1.4065**
C(1)-H(30)	1.1	1.1003	C(1)-C(2)	1.42	**1.3966**

Table 3. Dihedral angles of Gentian Violet dye.

Bond	**Actual (deg.)**	**Optimal(deg.)**	**Bond**	**Actual (deg.)**	**Optimal(deg.)**
C(28)-H(59)	1.113	1.1131	C(10)-H(34)	1.1	**1.1074**
C(28)-H(58)	1.113	1.1153	C(5)-H(33)	1.1	**1.0999**
C(28)-H(57)	1.113	1.1126	C(4)-H(32)	1.1	**1.0989**
C(27)-H(56)	1.113	1.116	C(2)-H(31)	1.1	**1.1011**
C(27)-H(55)	1.113	1.1136	C(1)-H(30)	1.1	**1.1003**
C(27)-H(54)	1.113	1.1117	N(21)-C(28)	1.47	**1.4799**
C(26)-H(53)	1.113	1.114	N(21)-C(27)	1.47	**1.4817**
C(26)-H(52)	1.113	1.1135	N(20)-C(26)	1.47	**1.4835**
C(26)-H(51)	1.113	1.1059	N(20)-C(25)	1.47	**1.4831**
C(25)-H(50)	1.113	1.1135	N(22)-C(24)	1.5	**1.5218**
C(25)-H(49)	1.113	1.1142	N(22)-C(23)	1.5	**1.5253**
C(25)-H(48)	1.113	1.1075	C(17)-N(22)	1.3	**1.3396**
C(24)-H(47)	1.113	1.1137	C(12)-N(21)	1.462	**1.4396**
C(24)-H(46)	1.113	1.1138	C(6)-N(20)	1.462	**1.4261**
C(24)-H(45)	1.113	1.1082	C(19)-C(9)	1.503	**1.4676**
C(23)-H(44)	1.113	1.1134	C(18)-C(19)	1.337	**1.3534**
C(23)-H(43)	1.113	1.1123	C(17)-C(18)	1.503	**1.4674**
C(23)-H(42)	1.113	1.1131	C(16)-C(17)	1.503	**1.4685**
C(19)-H(41)	1.1	1.1011	C(15)-C(16)	1.337	**1.3562**
C(18)-H(40)	1.1	1.1016	C(9)-C(15)	1.503	**1.4717**
C(16)-H(39)	1.1	1.1015	C(14)-C(8)	1.42	**1.408**
C(15)-H(38)	1.1	1.1002	C(13)-C(14)	1.42	**1.3963**
C(14)-H(37)	1.1	1.1071	C(12)-C(13)	1.42	**1.4088**
C(13)-H(36)	1.1	1.103	C(11)-C(12)	1.42	**1.4065**
C(11)-H(35)	1.1	1.1026	C(10)-C(11)	1.42	**1.3993**
C(3)-C(4)	1.42	1.4104	H(52)-C(26)-N(20)		**108.9852**
C(2)-C(3)	1.42	1.4065	H(51)-C(26)-N(20)		**116.2052**
C(1)-C(2)	1.42	1.3966	H(50)-C(25)-H(49)	109	**107.6514**
H(59)-C(28)-H(58)	109	108.8237	H(50)-C(25)-H(48)	109	**109.4898**
H(59)-C(28)-H(57)	109	110.5909	H(50)-C(25)-N(20)		**109.2201**

H(59)-C(28)-N(21)		110.6264	H(49)-C(25)-H(48)	109	**105.1682**
H(58)-C(28)-H(57)	109	105.7745	H(49)-C(25)-N(20)		**109.2382**
H(58)-C(28)-N(21)		107.7235	C(3)-C(4)	1.42	**1.4104**
H(57)-C(28)-N(21)		113.0675	C(2)-C(3)	1.42	**1.4065**
H(56)-C(27)-H(55)	109	108.591	C(1)-C(2)	1.42	**1.3966**
H(56)-C(27)-H(54)	109	105.7354	H(59)-C(28)-H(58)	109	**108.8237**
H(56)-C(27)-N(21)		107.688	H(59)-C(28)-H(57)	109	**110.5909**
H(55)-C(27)-H(54)	109	110.7194	H(59)-C(28)-N(21)		**110.6264**
H(55)-C(27)-N(21)		110.5839	H(52)-C(26)-N(20)		**108.9852**
H(54)-C(27)-N(21)		113.2644	H(51)-C(26)-N(20)		**116.2052**
H(53)-C(26)-H(52)	109	107.6064	H(50)-C(25)-H(49)	109	**107.6514**
H(53)-C(26)-H(51)	109	105.0736	H(50)-C(25)-H(48)	109	**109.4898**
H(53)-C(26)-N(20)		109.2958	H(50)-C(25)-N(20)		**109.2201**
H(52)-C(26)-H(51)	109	109.3199	H(49)-C(25)-H(48)	109	**105.1682**

Conclusions:

In this study, it was shown that a simple, available and inexpensive plant was used to remove dyes that pollute the environment, which is the stachy with a Gentian Violet dye. The adsorption process reached equilibrium in 25 minutes, according to the findings. As the adsorbent dose is raised, the amount of adsorbed dye increases, but after 0.3 g, the amount of adsorbed dye declines. At pH 3, the largest adsorption of (GV) was seen, while at pH 9, the lowest adsorption was observed. The increase in adsorption with increased ionic strength could be due to compression of the thickness of the diffused double layer. The second-order kinetic model had higher correlation coefficients than the first-order kinetic model. Study the theoretical electrostatics of Gentian Violet dye was measured and plotted as a 2D and 3D contour and The program hyperchem-8.07 was used for semi-empirical and molecular mechanic calculations in the gas phase to estimate the total energy.

Author's declaration:

- Conflicts of Interest: None.
- We hereby confirm that all the Figures and Tables in the manuscript are ours. Besides, the Figures and images, which are not ours, have been given permission for re-publication attached with the manuscript.
- Ethical Clearance: The project was approved by the local ethical committee in University of Baghdad.

Authors Contribution:

All authors contributed to the design and implementation of the research, to the analysis of the results and to the writing of the manuscript.

References:

1. Ebrahim A S, Tarek A F, Marwa N, Mohamed D. A Comparative Study for Adsorption of Methylene Blue Dyefrom Wastewater onto Three Different Types of Rice Ash. J Pharm Appl Chem. 2018; 4 (1): 99-107.
2. Haipeng Z, Mengjun C, Huan W, Zhenhua W, Jiajing C, Liu F, et al. Transcriptomic and metabolomic analyses provide insight into the volatile compounds of citrus leaves and flowers. BMC Plant Biol. 2020; 20(7): 1-14.
3. Ayed L, Chaieb K, Cheref A. Biodegradation of Triphenylmethane Dye Malachite Green By sphingomonas Paucimobilis. World J Microbiol. Biotechnol. 2009; 25(4): 705.
4. Mittal A, Mittal J, Malviya A, Gupta V K. Removal and recovery of Chrysoidine Y from aqueous solutions by waste materials. J Colloid Interface Sci. 2010; 344 (2): 497–507.
5. Alkaram F, Mukhlis A. The removal of phenol from aqueous solutions by adsorption using

surfactant-modified bentonite and kaolinite. J Hazard Mater. 2009; 169 (1-3): 324-332.

6. Sughosh M, Arif A, Amit K, Jyoti K, Joginder C, Sanjeev S, et al. Water pollutants: sources and impact on the environment and human health. Sensors in Water Pollutants Monitoring: Role of Material. Springer, Singapore, October. 2019;43-62.
7. Sandeep P, Sukanta M, Dilip K C, Chetan K D, Sanjay K S, Kumar A. Vinod. Effect of coal fly ash's particle size on U adsorption in water samples and thermodynamic study on adsorption. Environ Chem Ecotoxicol. 2020; 2. 32-38.
8. Tran H Tu , Phan Thi Ngoc Cam, Le Van Trong Huy , Mai Thanh Phong , Hoang Minh Nam,Nguyen Huu Hieu. Synthesis and application of graphene oxide aerogel as an adsorbent for removal of dyes from water. Mater Lett. 2018;238: 134-137.
9. Aljeboree Aseel M, Alshirifi Abbas N, Alkaim Ayad F. Kinetics and equilibrium study for the adsorption of textile dyes on coconut shell activated carbon. Arab J Chem. 2017; 10 (2): S3381–S3393.
10. ShanHo Y, Augustine E. Ofomaja. Kinetic studies of copper ion adsorption on palm kernel fibre .J Hazard Mater. 2006; 137 (3). 1796-1802.
11. Oğuzhan K, Bilal A. Adsorption of basic green 4 from aqueous solution by olive pomace and commercial activated carbon: process design, isotherm, kinetic and thermodynamic studies. Desalination Water Treat. 2016; 57 (35). 16653-16669.
12. Murugan T, Vasugi K, Praphakaran P, Prabhu P. A Study of Adsorption Dynamics of Biologically Active Plants. Int J Res Appl Eng Sci Tech. 2021; 9 (X): 1466- 1479.
13. Yasemin B, Haluk A. A kinetics and thermodynamics study of methylene blue adsorption on wheat shells. Desalination. 2006; January.194 (1–3). 259-267.
14. Cazetta AL, Vargas AM., Nogami EM., Kunita MH, Guilherme MR., Martins AC, et al. NaOH-activated carbon of high surface area produced from coconut shell: Kinetics and equilibrium studies from the methylene blue adsorption. Chem Eng J. 2011; 174 (1): 117–125.
15. Wanyonyi WC, Mmari JO, Mwanza PS. Adsorption of congo red dye from aqueous solutions using roots of eichhornia crassipes: kinetic and equilibrium studies. Energy Procedia. 2014; 2. 862 – 869.
16. Hameed BH, Mahmoud DK. Sorption of basic dye from aqueous solution by pomelo (Citrus grandis) peel in a batch system .Colloids Surf A Physicochem Eng Asp. 2008; March. 316 : (1–3). 78-84.
17. Karla A G, Leandro VA, Tânia Márcia SM, Laurent FG. Adsorption studies of methylene blue and gentian violet on sugarcane bagasse modified with EDTA dianhydride (EDTAD) in aqueous solutions: Kinetic and equilibrium aspects. J Environ Manage. 2013; 30 (118): 135- 143.
18. Indra D M , Vimal C S, Nitin K A, Indra M M. Removal of congo red from aqueous solution by bagasse fly ash and activated carbon: kinetic study and equilibrium isotherm analyses. Chemosphere. 2005; 61 (4): 492-501.
19. Jain R, Shrivastava M. Adsorptive studies of hazardous dye Tropaeoline 000 from an aqueous phase onto coconut-husk. J Hazard Mater. 2008; 158 (2-3): 549–556.
20. Shaymaa K G, Intidhar D S, Najwa I A. Adsorption of Congo Red Dye from Aqueous Solution onto Natural and Modified Bauxite Clays. Baghdad Sci J. 2017; March. 14(1): 167-180. https://doi.org/10.21123/bsj.2017.14.1.0167
21. Khulood A, Dunya E, Huda N. Using Phragmites australis (Iraqi plant) to remove the Lead (II) Ions form Aqueous solution. Baghdad Sci J. 2017; March. 14(1): 148- 156. https://doi.org/10.21123/bsj.2017.14.1.0148
22. Hameed, KS, Muthirulan, P, Meenakshi, SM. Adsorption of chromotrope dye onto activated carbons obtained from the seeds of various plants: Equilibrium and kinetics studies. Arabian J Chem. May. 2017; 10 (2): S2225–S2233.
23. Malik RR, DS, Wate SR. Adsorption of malachite green on groundnut shell waste based powdered activated carbon. J Waste Manage. 2007; 27 (9): 1129–1138.
24. Ahlam M. F, Ahlam M Z, Hussein I A. Adsorption Study of Rhodamine –B Dye on Plant (Citrus Leaves). Baghdad Sci J. 2022; January.4: 838- 847.
25. Inaam H A, Removal of Congo Red Dye From Aqueous Solution Using Eco-Friendly Adsorbent of Nanosilica. . Baghdad Sci J. 2021; January.18 (2): 366- 373.
26. Figgis, B, Hitchman M. Ligand Field Theory and Its Applications. John-Weily Heyden. 2000; Ltd, New York, London, 225 pp.

دراسة حركية ونظرية لأزالة صبغة جنتل فايولوت من محاليلها المائية بأستخدام نبات البطنج

زهراء عادل محمود* **احلام محمد فرحان** **نفيسة جبار كاظم** **منى سمير هادي**

قسم الكيمياء، كلية العلوم للبنات, جامعة بغداد, بغداد, العراق.

الخلاصة:

اجريت في هذا البحث دراسة امتزاز صبغة Gentian Violet على سطح نبات البطنج من محاليلها المائية. وفحص سطح النبات بواسطة تقنية FTIR, كما وتم دراسة تأثير كل من وقت الامتزاز ووزن المادة المازة والشدة الأيونية و pHعند درجة حرارة 289 كلفن. فقد ثبتت ان زيادة القوة الايونية تعمل على تحسين كمية الامتزاز. ودرست حركيات الامتزاز وثابت الاتزان وتطبيق معادلة لانكماير وفريدنليش وتمكن حيث اعطيت نتائج افضل بتطبيق معادلة تمكن. وتحديد ثابت سرعة التفاعل من خلال معالجة البيانات بمعادلات الحركية من الدرجة الاولى والثانية الكاذبة وبينت النتائج ان حركية الامتزاز تتبع معادلة المرتبة الثانية الكاذبة حيث ان قيمة $R^2= 0.\ 0.9943$.

الكلمات المفتاحية: امتزاز، جنتل فايوليت, حركية, نبات البطنج, معادلة تمكن.